

圆管状内壁面管口辐射传递的方向分布特性

路义萍, 李炳熙, 阮立明, 谈和平

(哈尔滨工业大学能源科学与工程学院, 黑龙江 哈尔滨 150001)

摘 要: 为了得到圆管状内壁面通过管口辐射传递的方向分布特性, 给出了圆管状内壁面单元间辐射传递系数 RD 的蒙特卡罗求解方法, 研究了当内壁为等温灰体、漫发射、漫反射时, 管内壁发射率、管长与半径比的变化对管口表面当量定向发射率的影响, 结果表明: 总趋势为管长与半径比增加, 管口表面当量定向发射率极值点向小角度的天顶角方向移动, 在管长与半径比较大时, 随管长增加, 管内壁发射率 ϵ 减小, 管出口表面较小天顶角方向当量定向发射率增大。

关 键 词: 辐射传热; 蒙特卡罗法; 圆管; 当量定向发射率

中图分类号: TK124 文献标识码: A

1 引 言

工业加热设备中有许多圆管状的元件, 如多孔燃气辐射器的单个小孔^[1]、燃烧器的管状元件部分^[2]等。当孔管内高温燃气流过时, 可以把气体介质当作透明体, 而只考虑孔管内表面单元间辐射换热, 这时换热属于辐射、对流非线性边界条件下的管壁内部的导热问题, 是较复杂的耦合换热计算。当采用蒙特卡罗法计算辐射换热时, 需计算辐射传递系数 RD 值^[3], 将计算的难点分离: 将面元的几何特性与辐射物性等与温度分离, 从而使辐射传递系数在能量方程(温度场)求解过程中保持不变, 或当辐射物性随温度变化时作微小的变动。辐射传递系数与能量方程的求解分离, 只与所研究孔管内壁的辐射热物性和几何尺度有关。限于目前的测试手段, 多数材料的辐射物性在很宽的温度区间变化很小, 可以认为辐射热物性不随温度变化, 辐射传递系数与温度无关。采用蒙特卡罗法计算该系数时, 模拟能束数为 1 000 万, 模拟量很大, 提高了计算精度。在计算 RD 值的过程中, 一部分能束通过孔管的管口射向环境直接加热被加热物体, 由于辐射本身的方向特性, 会导致加热不均匀现象, 所以有必要研究圆管状元件内壁面通过管口射出能束的方向分布特

性。文献 [1] 中假设小孔的内壁为黑体, 利用角系数计算管内壁单元间的相互投射辐射, 本文中给出了圆管内壁面单元之间辐射传递系数的蒙特卡罗求解方法; 研究了当管内壁为等温灰体、漫发射、漫反射时射出管口的辐射能的方向分布特性, 并用管口表面当量定向发射率来表示。

2 蒙特卡罗法研究过程描述

2.1 发射点位置的确定

发射点位置分布应符合在单元体区域内均匀分布的特点^[4]。圆管内壁面发射点位置 x, y, z 为:

$$\begin{aligned} x &= x_0 + R_x \Delta x \\ y &= Rc \cdot \sin \varphi \\ z &= Rc \cdot \cos \varphi \\ \varphi &= R_\varphi \cdot 2\pi \end{aligned} \quad (1)$$

式中: Rc 是圆柱的半径, R_x, R_φ 是 0 ~ 1 之间的均匀随机数, φ 为周向角。

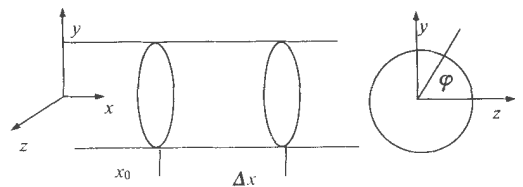


图 1 圆柱面发射点的确定

2.2 发射方向的确定

发射方向的确定采用两个坐标系 — 系统坐标 $oxyz$ 和动态坐标 $ox'y'z'$ 。系统坐标在圆管的左侧面 $x = 0$ 处, 动态坐标则由发射点位置决定。壁面为漫发射、漫反射的灰体, 概率模拟服从兰贝特定律^[6~7]。

对圆柱内壁面取如图 2 所示动态坐标系 $ox'y'z'$ 。则能束在动态坐标系下发射方向为:

$$\varphi = 2\pi R_\varphi \quad (2)$$

收稿日期: 2003-01-19; 修订日期: 2003-03-28

基金项目: 哈尔滨工业大学校内博士启动基金资助项目 (01502349)

作者简介: 路义萍 (1965—), 女, 黑龙江佳木斯人, 哈尔滨工业大学博士研究生, 现在哈尔滨理工大学工作, 副教授。

$$\theta = \cos^{-1} \sqrt{1 - R_0} \quad (3)$$

能束在动态坐标系下的空间参数直线方程为:

$$\begin{aligned} x' &= t \cos \alpha \\ y' &= t \cos \beta \\ z' &= t \cos \gamma \end{aligned} \quad (4)$$

式中: t 是有向线段的长度, $\cos \alpha$ 、 $\cos \beta$ 、 $\cos \gamma$ 为此向量在动态坐标系下的方向余弦, 由图 2 可知。

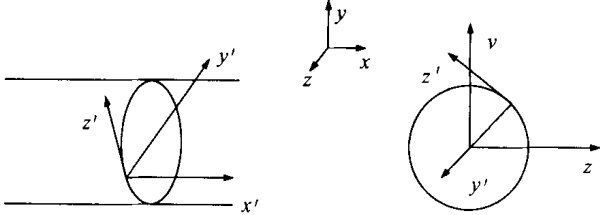


图 2 圆柱内表面能束发射方向的确定

$$\begin{aligned} \cos \alpha &= \sin \theta \sin \varphi \\ \cos \beta &= \cos \theta \\ \cos \gamma &= \sin \theta \cos \varphi \end{aligned} \quad (5)$$

将动态坐标系下直线方程转换成系统坐标系下直线方程, 设 i, j, k 是系统坐标系的基本向量; i', j', k' 是动态坐标系的基本向量。两个基本向量之间夹角如表 1 所示, 用 (x_0, y_0, z_0) 表示动态坐标系原点在系统坐标系下的坐标。

由空间解析几何知:

$$\begin{aligned} x &= x' \cos \alpha_1 + y' \cos \alpha_2 + z' \cos \alpha_3 + x_0 \\ y &= x' \cos \beta_1 + y' \cos \beta_2 + z' \cos \beta_3 + y_0 \\ z &= x' \cos \gamma_1 + y' \cos \gamma_2 + z' \cos \gamma_3 + z_0 \end{aligned} \quad (6)$$

由图 2 可知: 表 1 所示的动态坐标系与系统坐标系关系矩阵:

$$\begin{aligned} \cos \alpha_1 &= 1 & \cos \alpha_2 &= 0 & \cos \alpha_3 &= 0 \\ \cos \beta_1 &= 0 & \cos \beta_2 &= -y / \sqrt{y^2 + z^2} \\ \cos \beta_3 &= z / \sqrt{z^2 + y^2} \\ \cos \gamma_1 &= 0 & \cos \gamma_2 &= -z / \sqrt{z^2 + y^2} \\ \cos \gamma_3 &= -y / \sqrt{z^2 + y^2} \end{aligned} \quad (7)$$

表 1 动态坐标与系统坐标关系

	i	j	k
i'	α_1	β_1	γ_1
j'	α_2	β_2	γ_2
k'	α_3	β_3	γ_3

由式(4)、式(6)和式(7) 可得出能束向量在系统坐标系下参数方程

2.3 接收点坐标的确定

当发射能束的直线方程确定后, 需判断能束与圆柱内表面交点位置。

圆柱方程:

$$y^2 + z^2 = R^2 \quad 0 \leq x \leq xl \quad (8)$$

将能束直线式(6) 代入式(8), 可得到关于空间向量长度 t 的二次方程。当发射点位于圆柱内时, t 值必须为正, 且满足式(8) 和所表达的 x 取值范围, 将求出的 t 值反代入式(6), 即可求得交点的位置。否则, 从管口射出, 式中: xl 为圆柱长度。

2.4 RD 值计算

沿管长方向划分为 n 个单元, $n = xl / \Delta x$, $\Delta x = Rc$ 。当管内壁发射单元 i 和到达管内壁单元 j 确定后, 便可计算出辐射传递系数 RD 值^[7]。根据蒙特卡罗法: 取任一随机数 R , 当 R 小于管内壁面黑度 ϵ 时, 能束被吸收, N_j 累计加 1; 当 $R > \epsilon$ 时, 能束不被吸收, 则将到达点 j 作为新的发射点, 重新计算发射方向及新一轮到达点。跟踪这一能束直到它被吸收或逸出圆柱区域。如果逸出, 研究能束离开方向分布, 相对管口表面法向天顶角 θ 平均分为 m 份, j 表示管出口表面第 j 个天顶角空间单元, 累计 i 单元发射第 j 个天顶角空间单元逸出的能束数 N_{ij} , 从管内壁 i 单元发射管口表面第 j 个天顶角 θ 处逸出的辐射传递系数也计为: $RD(i, j)$ 。 N_i 为 i 单元表面发射的能束总数, 取 1 000 万。可得:

$$RD(i, j) = N_{ij} / N_i \quad (9)$$

3 圆管出口逸出能束方向性确定

3.1 管出口表面逸出能束方向性数学描写

利用前面介绍的计算 RD 的方法计算圆管内壁从管口射向环境的能束的方向分布特性。对于圆柱形管子左右侧管口基于管中心线位置是对称的, 本文研究右侧(见图 3 管出口表面当量定向发射率研究示意图)。当能束逸出管口时, 定向发射率应为能束逸出位置、逸出时相对管表面的周向角与天顶角的函数 $\epsilon(r, \varphi, \theta)$, 当管径很小时, 不考虑从管口逸出的位置, 认为是从中心管轴线处逸出, 沿圆周方向具有对称性, 周向射出的能束应为均匀的, 因而定向发射率仅为天顶角 θ 的函数。相对管口表面法向 θ 角平均分为 90 份, $\Delta\theta = 1^\circ$ 。为了表示不同天顶角间辐射强度的相对大小, 本文定义管出口表面当量定向发射率 $\epsilon(\theta)$;

$$\epsilon(\theta) = \frac{I_0}{I_{ap}} \quad (10)$$

其中: $I(\theta) = \frac{\sum_{i=1}^n RD(i, j) \cdot E_i \cdot A_i}{\pi(Rc)^2 \int_{(j-1)\Delta\theta}^{j\Delta\theta} \int_0^{2\pi} \sin\theta \cdot \cos\theta \cdot d\theta \cdot d\varphi}$ (11)

式(11)中 E_i, A_i 分别为第 i 个内壁面单元的辐射力、辐射面积, $j = 1 \sim m$ 。

定义管口当量辐射强度: $I_{ap} =$
管口逸出总辐射能
管口表面面积 $\cdot \pi$

在等温、等发射率和等单元面积时, 化简后式(10)变为:

$$\epsilon(\theta) = \frac{\sum_{i=1}^n RD(i, j)}{(\cos^2(\Delta\theta(j-1)) - \cos^2(\Delta\theta \cdot j)) \sum_{j=i=1}^m \sum_{i=1}^n RD(i, j)} \quad (12)$$

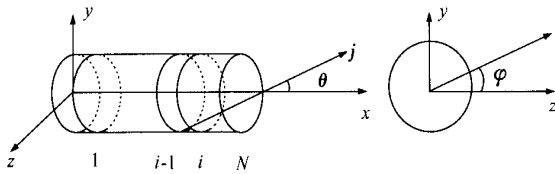


图3 管出口表面当量定向发射率研究示意图

3.2 圆管管口逸出能束当量定向发射率计算及分析

本文分别计算了管长与半径比 xL/Rc 分别为 4、10、20、30, 内壁面发射率为 0.2、0.8 时辐射传递系数 $RD(i, j)$ 、管口表面当量定向发射率 $\epsilon(\theta)$ 的数值。

表 2 给出了 $xL/Rc = 10, \epsilon = 0.8$ 沿管长方向分成 10 个单元时, 发射单元 i 在圆形管右侧出口处的天顶角区间 j 逸出的辐射传递系数, $i = x/Rc$, 管右侧出口表面天顶角 $\theta = j(\Delta\theta), \Delta\theta = 15^\circ$ 。分析表 2 可以得出: 离管口越近 ($i = 10$), 管口表面能束逸出

表 2 $\epsilon = 0.8$, 管长与半径比 $xL/Rc = 10$ 时, 圆管右侧出口辐射传递系数随发射单元位置 i 、管出口表面的天顶角位置 $j(j = 1 \sim 6, \Delta\theta = 15)$ 变化数据

$RD(i, j)$	$i = 1$	$i = 2$	$i = 3$	$i = 4$	$i = 5$	$i = 6$	$i = 7$	$i = 8$	$i = 9$	$i = 10$
$\theta = 0 - 15$	0.0013	0.0020	0.0028	0.0035	0.0045	0.0055	0.0067	0.0082	0.0116	0.0207
$\theta = 15 - 30$	0.0000	0.0000	0.0000	0.0005	0.0023	0.0062	0.0154	0.0264	0.0405	0.0712
$\theta = 30 - 45$	0.0000	0.0000	0.0000	0.0000	0.0000	0.0000	0.0006	0.0144	0.0531	0.1041
$\theta = 45 - 60$	0.0000	0.0000	0.0000	0.0000	0.0000	0.0000	0.0000	0.0000	0.0225	0.1002
$\theta = 60 - 75$	0.0000	0.0000	0.0000	0.0000	0.0000	0.0000	0.0000	0.0000	0.0004	0.0541
$\theta = 75 - 90$	0.0000	0.0000	0.0000	0.0000	0.0000	0.0000	0.0000	0.0000	0.0000	0.0086

天顶角度范围越大, 离管口越远, 能束逸出时天顶角度范围越小, 计算结果表明: $i = 1 \sim 3$ 时, 能束逸出时落在天顶角 $\theta < 15^\circ$ 范围, $i = 4 \sim 6$ 时, 能束逸出时落在天顶角 $\theta < 30^\circ$ 范围。出口处能束在不同天顶角范围内的辐射传递系数 $RD(i, j)$ 份额随管长变化特性, 直接导致管出口表面辐射强度随天顶角变化。

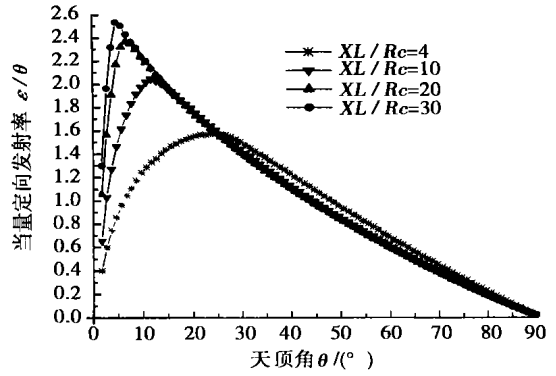


图4 管内壁发射率 $\epsilon = 0.2$ 时, 管右侧出口 $\epsilon(\theta)$ 随 $xL/Rc, \theta$ 变化曲线

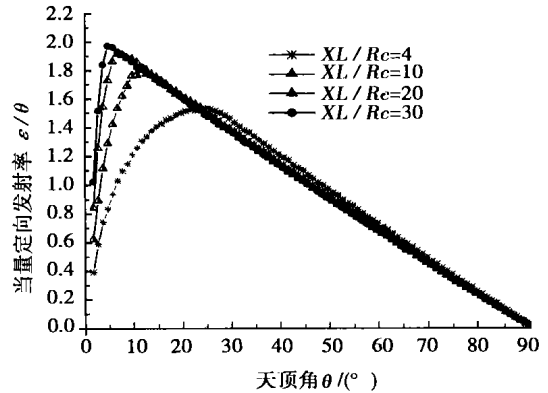


图5 管内壁发射率 $\epsilon = 0.8$ 时, 管右侧出口 $\epsilon(\theta)$ 随 $xL/Rc, \theta$ 变化曲线

图 4 和图 5 分别给出了管内壁等温时管出口表面当量定向发射率 $\epsilon(\theta)$ 随管内壁发射率 ϵ 、管长与半径比 (xl/Rc) 的变化曲线。由图中的曲线可发现:

- (1) 管出口当量定向发射率 $\epsilon(\theta)$ 出现极大值;
- (2) 随管长与半径比的增加, 最大当量定向发射率 $\epsilon(\theta)$ 所对应的天顶角 θ 向较小角度方向移动; 该极大值随 xl/Rc 增大而增大。但是 xl/Rc 大于 20 以后, xl/Rc 的增大对 $\epsilon(\theta)$ 影响较小。

由图 4 和图 5 比较可看出: 管长与半径比 ($xl/Rc = 4$) 较小时, 管内壁发射率 ϵ 对管口当量定向发射率的影响不显著 ($xl/Rc = 4, \epsilon = 0.8, 0.2$ 时最大当量定向发射率分别为 1.53、1.57); 随 xl/Rc 增加 (xl/Rc 大于 10), ϵ 小时, 管内壁发射率 ϵ 对管口当量定向发射率的影响非常明显 ($xl/Rc = 10, \epsilon = 0.8, 0.2$ 时最大当量定向发射率分别为 1.80 和 2.04; $xl/Rc = 20, \epsilon = 0.8, 0.2$ 时最大当量定向发射率分别为 1.91 和 2.37)。

4 结 论

- (1) 管出口当量定向发射率不管 xl/Rc 多大, 都存在极大值, 但其最大值随 xl/Rc 增大而增大;
- (2) 最大当量定向发射率对应天顶角 θ 随着

xl/Rc 的增大向小角度天顶角方向移动, 但当 xl/Rc 大于 20 以后, 增加的数值较小。

- (3) 在管长与半径比大于 4 时, 管内壁发射率 ϵ 对管口当量定向发射率的影响显著, 随着 xl/Rc 的增大 ϵ 减小, 从管口逸出的辐射能集中在天顶角较小的空间范围, 其定向性越好。

参考文献:

- [1] 李艳红, 徐吉洸, 张鹤声. 多孔陶瓷板中城市煤气预混燃烧的实验研究与数值模拟[J]. 工程热物理学报, 1997, 18(3): 385—388.
- [2] 王承炜. 径向浓淡旋流燃烧器扩锥温度场数值模拟[D]. 哈尔滨: 哈尔滨工业大学, 1999.
- [3] YANG W J, HIROSHI TANIGUCHI, KAZUHIKO KUDO. Radiative heat transfer by the monte carlo method [M]. California: Academic Press Inc, 1995.
- [4] HOWELL J R. The monte carlo method in radiative heat transfer [J]. **Journal of Heat Transfer**, 1998, 120(3): 547—560.
- [5] MODEST M F. Radiative heat transfer [M]. New York: McGraw—Hill Inc, 1993.
- [6] SIEGEL R, HOWELL J R. Thermal radiation heat transfer [M]. New York: Taylor & Francis, 2002.
- [7] 谈和平, 崔国民, 阮立明, 等. 用区域分解算法结合蒙特卡罗法求坦克温度场和红外辐射出射度[J]. 工程热物理学报, 1998, 19(3): 340—344.

(何静芳 编辑)

(上接第 16 页)

参考文献:

- [1] 钱颂文, 岑汉钊, 曾文明. 换热器流体诱导振动[M]. 北京: 烃加工出版社, 1989.
- [2] 卢家才, 谢正武, 林宗虎, 等. 气液两相流中旋涡诱发圆柱振动时的脉动升力研究[J]. 应用力学学报, 1999, 16(3): 20—25.
- [3] 谢正武, 苏新军, 林宗虎, 等. 气液两相流诱发顺列双圆柱升力功率谱特性研究[J]. 西安交通大学学报, 1999, 33(8): 28—31.
- [4] 苏新军, 张修刚, 林宗虎. 错列圆柱表面周向压力分布的试验研究[J]. 西安交通大学学报, 2001, 35(1): 1—4.
- [5] 苏新军, 牛冬梅, 林宗虎. 气液两相流中错列管束上脉动升力的试验研究[J]. 西安交通大学学报, 2000, 34(11): 9—12.
- [6] 苏新军. 气液两相旋涡脱落时错列管束受力的实验研究[D]. 西安: 西安交通大学能源与动力工程学院, 1999.
- [7] GUNTER S. On the force fluctuations acting on a circular cylinder in

crossflow from subcritical up to transcritical reynolds numbers[J]. **J Fluid Mech**, 1983, 133(8): 265—285.

- [8] RICHTER A, NAUDASCHER E. Fluctuating forces on rigid circular cylinder in confined flow[J]. **J Fluid Mech**, 1976, 78(3): 561—576.
- [9] WEAVER D S, FITZPATRICK J A. A review of cross-flow induced vibrations in heat exchanger tube arrays[J]. **Journal of Fluids and Structures**, 1988, 10(2): 73—93.
- [10] 白菜文斯 R D. 流体诱导振动[M]. 北京: 机械工业出版社, 1983.
- [11] 林宗虎. 气液两相流和沸腾传热[M]. 西安: 西安交通大学出版社, 1987.
- [12] WEAVER D S, FITZPATRICK J A, ELKASHL H. Strouhal numbers for heat exchanger tube arrays in cross flow[J]. **Flow Induced Vibration**, 1986, 104: 193—200.

(何静芳 编辑)

non-dimensionalized treatment. On the basis of an invariance principle of differential equations similarity criteria were deduced, which the humidifier shall comply with during the experimental research. Some explanations are given concerning the role being played by these criteria during experiments. Moreover, some major issues requiring due attention during the tests of the humidifier are also presented. **Key words:** humid air turbine cycle, humidifier, heat and mass transfer, similarity analysis

等截面直肋传热简化计算的适用条件 = **Applicable Conditions for the Simplified Calculation of Heat Transfer for Straight Fins of Uniform Cross-section** [刊, 汉] / XU Zhi-ming, ZHOU Li-qun, BU Yu-bing, et al (Northeast Electric Power Institute, Jilin, China, Post Code: 132012) // Journal of Engineering for Thermal Energy & Power. - 2004, 19(1). - 42 ~ 44

With the help of a theoretical analysis method a fin-end adiabatic calculation formula is often used instead of a formula based on a fin-end convection heat exchange to calculate the heat transfer of straight fins of uniform cross-section. The approximate error thus obtained can be expressed as a function of the ratio of cross-sectional area to lateral area $f/(Uh)$ and also as a function of Biot number Bi . Through a calculation of the possible range of selected values it has been found that when one of the following two conditions is met, the error of the above calculation method will be less than 1%. The two conditions are 1. The ratio of $f/(Uh)$ of the straight fins is less than 0.5; 2. Number Bi is greater than 7. **Key words:** assumed fin height, Biot criteria, the ratio of cross-sectional area to lateral area

相变材料相变点温度热物性的测试及误差分析 = **Test Measurements and Error Analysis of Thermo-physical Properties of Phase-change Materials at a Phase-transition Point Temperature** [刊, 汉] / LI Chang-geng, ZHOU Jie-min (Institute of Physical Sciences under the Zhongnan University, Changsha, China, Post Code: 410083) // Journal of Engineering for Thermal Energy & Power. - 2004, 19(1). - 45 ~ 47

The moving phase-interface curves during a solid-liquid phase-transition process are closely related with such a variety of two-phase thermo-physical properties as specific heat, density, thermal conductivity and phase-transition latent heat. The authors have come up with a method for determining several thermo-physical parameters, among others, the thermal conductivity of phase-change materials at a solid-liquid phase transition temperature. The above determination was carried out through the measurement of phase-interface moving rates. A test measurement device was designed and a quantitative analysis of measurement errors performed of the test measurement system. It was found that the error of the measurement system based on a combination of numerical calculations and experimental tests would not exceed 3%. The thermal conductivity and thermal diffusion factor of several kinds of materials were measured by using the above-mentioned test measurement system with satisfactory results being obtained. This shows that the measurement method proposed by the authors is trustworthy. **Key words:** phase change materials, thermo-physical properties, measurement, error analysis

圆管状内壁面管口辐射传递的方向分布特性 = **Direction Distribution Characteristics of Radiation Transmission from a Cylindrical Inner-wall Surface Tube-end** [刊, 汉] / LU Yi-ping, LI Bing-xi, YUAN Li-ming, et al (Institute of Energy Science and Engineering under the Harbin Institute of Technology, Harbin, China, Post Code: 150001) // Journal of Engineering for Thermal Energy & Power. - 2004, 19(1). - 48 ~ 51

To obtain the direction distribution of radiation transmission through the tube end of a cylindrical inner-wall surface the authors have introduced a Monte Carlo method for solving the radiation transmission factor RD among cylindrical tube inner-wall surface elements. With the inner wall being an isothermal gray body, of a diffuse emission and diffuse reflection the impact was studied of the change of tube inner-wall emission rate, and of the ratio of tube length to radius on the equivalent directional emission rate of a tube-end surface. The study results indicate the following general tendency. With the increase in tube length-to-radius ratio the maximum value point of the equivalent directional emission rate of the tube-end surface will shift in the direction of a small-angled zenith angle. When the ratio of tube length to radius is relatively great, the tube inner-wall emission rate will decrease with an increase in tube length. With a relatively small tube outlet

surface the equivalent orientation emission rate in the zenith angle direction will increase. **Key words:** radiation heat transfer, Monte Carlo method, tube, equivalent orientation emission

分级燃烧对固体吸附剂吸附痕量金属的影响= **The Impact of Graded Combustion on the Adsorption of Trace Metals by Solid Adsorbents** [刊, 汉] / HAN Jun, XU Ming-hou, ZENG Han-cai, et al (National Key Laboratory of Coal Combustion under the Huazhong University of Science & Technology, Wuhan, China, Post Code: 430074) // Journal of Engineering for Thermal Energy & Power. — 2004, 19(1). — 52 ~ 55, 58

An experimental investigation was carried out in an one-dimensional pulverized-coal furnace to study the impact of graded combustion on the control by adsorbents of the emission of heavy metals. Through the investigation it was found that the graded combustion would increase the concentration of heavy metals in sub-micron particles, which is unfavorable for the control of trace heavy metals. This influence is especially significant in the case of highly volatile elements, such as copper and nickel. Solid adsorbents play an adsorption role with respect to the emission of heavy metals present in coal. Moreover, the adsorbents have a selective tendency in the adsorption of different heavy metals. In conclusion, the authors have expounded the mechanism of adsorption of heavy metal elements by the adsorbents. Such a mechanism is realized through both a physical and chemical adsorption, which coexist during a adsorption process. **Key words:** trace heavy metal, graded combustion, adsorbent, coal combustion

催化重整反应对柴油掺水燃烧中着火的影响= **The Influence of a Catalytic Reforming Reaction on the Ignition of Diesel Oil Mixed with Water** [刊, 汉] / WANG Chao, GONG Jing-song, FU Wei-biao (Department of Engineering Mechanics, Tsinghua University, Beijing, China, Post Code: 100084) // Journal of Engineering for Thermal Energy & Power. — 2004, 19(1). — 56 ~ 58

The impact of a catalytic reforming reaction on the ignition temperature was investigated during the firing of diesel oil mixed with water. The focus of the investigation is on the change of ignition temperature when the catalytic reforming reaction takes place or not. From the results of experiments it can be seen that the catalytic reforming reaction has a significant influence on the ignition of emulsified diesel oil and can markedly reduce the ignition temperature. A detailed description is given of the experimental devices, test process and results along with circumstantial explanations and analyses. It is concluded that the catalytic reforming reaction can lower the ignition temperature of the emulsified diesel oil. Furthermore, two conditions essential for the implementation of catalytic reforming are also put forward. **Key words:** emulsified diesel oil, catalysis, reforming reaction, ignition

成型压力和炉膛温度对单颗粒型煤燃烧失重特性的影响= **The Impact of Forming Pressure and Furnace Temperature on the Weight-loss Characteristics of Single-particle Briquette Combustion** [刊, 汉] / DONG Peng, JIANG Xue-hui, ZHAO Guang-bo (College of Energy under the Harbin Institute of Technology, Harbin, China, Post Code: 150001) // Journal of Engineering for Thermal Energy & Power. — 2004, 19(1). — 59 ~ 62

By making use of a thermogravimetric analysis method the weight-loss characteristics of single-particle briquette combustion were investigated. As a result, the laws governing the impact of forming pressure and furnace temperature on the weight-loss characteristics of single-particle briquette combustion have been deduced. In combination with a theoretical analysis a mathematical model was set up, which can reflect the mechanism of this influence. **Key words:** briquette, combustion, thermogravimetric analysis

蜂窝陶瓷蓄热体格孔壁面应力变化特性的数值研究= **Numerical Study of the Stress Variation Characteristics at the Cellular-hole Wall-surface of a Honeycomb Ceramic Regenerator** [刊, 汉] / OU Jian-ping, JIANG Shao-jian, XIAO Ze-qiang (Institute of Energy & Power Engineering under the Zhongnan University, Changsha, China, Post Code: 410083), WU Chuang-zhi (Guangzhou Energy Source Research Institute under the Chinese Academy of Sciences, Guangzhou, China, Post Code: 510070) // Journal of Engineering for Thermal Energy & Power. — 2004, 19(1). — 63